Collective excitations of Dirac electrons in a graphene layer with spin-orbit interactions

Xue-Feng Wang and Tapash Chakraborty*
Department of Physics and Astronomy, The University of Manitoba, Winnipeg, Canada R3T 2N2
(Received 22 May 2006; revised manuscript received 13 November 2006; published 16 January 2007)

Coulomb screening and the excitation spectra of electrons in a graphene layer with spin-orbit interaction (SOI) are studied in the random phase approximation. The SOI opens a gap between the valence and conduction bands and between the intraband and interband electron-hole excitation continuum of the semimetal Dirac system. As a result, we have observed a dramatic change in the long-wavelength dielectric function of the system. An undamped plasmon mode appears in the electron-hole continuum gap reflecting the interplay between the intraband and interband electron correlations.

DOI: 10.1103/PhysRevB.75.033408 PACS number(s): 73.21.−b, 71.70.Gm, 75.10.Lp, 75.70.Ak

Ever since the recent discovery of the quantum Hall effect in graphene,[1–3] there has been an upsurge of interest in understanding its electronic properties. Graphene has a promising potential for nanoscale device applications[4] and is also very interesting physically because of its unusual Dirac-Weyl type band-structure near the Fermi level.[5–11] As a single layer of graphite or an unrolled single-walled nanotube, the energy band structure of graphene is well known just as for the graphite or for a nanotube.[5,6,8] Past few years have evidenced increased activities in the role of the spin-orbit interaction (SOI) in nanostructures because it introduces many unusual features in these systems. The SOI is also predicted to exhibit interesting effects such as the spin Hall effect in graphene[8] but overall its effect in graphene is as yet, unclear.[12] Further, the electron-electron interaction is also important to understand the behavior of electrons in graphene and has been studied by many authors in graphite-based structures but without the SOI included.[12–15] In this paper, we explore the effect of the SOI on the electron-electron interaction and the characteristic excitations in a graphene layer.

Graphene has a honeycomb lattice of carbon atoms with two sublattices. Its energy band can be calculated by the tight-binding model[5,6] and an intrinsic graphene is a semimetal with the Fermi energy located at the inequivalent K and K' points at opposite corners of its hexagonal Brillouin zone.[5] In the effective mass approximation, the Hamiltonian of electrons near the Fermi energy is expressed by a 8×8 matrix. Since the SOI due to the atomic potential only mixes the states corresponding to the two sublattices, we can reduce the matrix to four independent 2×2 blocks. In the representation of the two sublattices, the Hamiltonian of a spin-up electron near the K point of the reciprocal space reads[8,9]

$$H = v\boldsymbol{p}\cdot\sigma + \Delta_{\mathrm{SO}}\sigma_z = \begin{bmatrix} \Delta_{\mathrm{SO}} & -i\hbar v\nabla^- \\ -i\hbar v\nabla^+ & -\Delta_{\mathrm{SO}} \end{bmatrix}, \tag{1}$$

with $\sigma=(\sigma_x,\sigma_y,\sigma_z)$ the Pauli matrices in the pseudospin space of the two sublattices and $\nabla^{\pm}=\partial/\partial x \pm i\partial/\partial y$. Here $v=10^6$ m/s is the "light" velocity of the Dirac electron gas and Δ_{SO} is the strength of the spin-orbit interaction. The eigenfunction are $\Psi_{\boldsymbol{k}}^{+}(\boldsymbol{r})=e^{i\boldsymbol{k}\cdot\boldsymbol{r}}\begin{pmatrix}\cos(\alpha_k/2)\\ e^{i\phi_k}\sin(\alpha_k/2)\end{pmatrix}$ for the state $|\boldsymbol{k},+\rangle$ in the conduction band of energy $E_{\boldsymbol{k}}^{+}=\sqrt{\Delta_{\mathrm{SO}}^2+\hbar^2v^2k^2}$ while $\Psi_{\boldsymbol{k}}^{-}(\boldsymbol{r})=e^{i\boldsymbol{k}\cdot\boldsymbol{r}}\begin{pmatrix}\sin(\alpha_k/2)\\ -e^{i\phi_k}\cos(\alpha_k/2)\end{pmatrix}$ for the state $|\boldsymbol{k},-\rangle$ in the valence band $E_{\boldsymbol{k}}^{-}=-\sqrt{\Delta_{\mathrm{SO}}^2+\hbar^2v^2k^2}$ with $\tan\phi_{\boldsymbol{k}}=k_y/k_x$, $\tan\alpha_k=\hbar vk/\Delta_{\mathrm{SO}}$, and $k=\sqrt{k_x^2+k_y^2}$. For a bare Coulomb scattering of two electrons at states $|\boldsymbol{k},\lambda\rangle$ and $|\boldsymbol{p},\lambda_1\rangle$ into states $|\boldsymbol{k}+\boldsymbol{q},\lambda'\rangle$ and $|\boldsymbol{p}-\boldsymbol{q},\lambda_1'\rangle$, respectively, the interaction matrix elements are

$$v_{\boldsymbol{k},\boldsymbol{p}}^{\lambda,\lambda',\lambda_1,\lambda_1'} = g_{\boldsymbol{k}}^{\lambda,\lambda'}(\boldsymbol{q})v_0(q)g_{\boldsymbol{p}}^{\lambda_1,\lambda_1'}(-\boldsymbol{q}). \tag{2}$$

Here $v_0=e^2/(2\epsilon_0\epsilon_i q)$ is the two-dimensional Coulomb interaction (in the Fourier space) with the high-frequency dielectric constant $\epsilon_i=1$[11], $g_{\boldsymbol{k}}^{\lambda,\lambda'}(\boldsymbol{q})$ is the interaction vertex, and the index $\lambda=\pm$ denotes the two bands. The randon-phase approximation (RPA) dressed interaction matrix elements have the same form as the bare interaction matrix elements, i.e., Eq. (2).[16] The dielectric matrix is then expressed as a unit matrix multiplied by a dielectric function

$$\hat{\epsilon}(q,\omega) = 1 - v_0(q)\hat{\Pi}_0(\boldsymbol{q},\omega) \tag{3}$$

with the electron-hole propagator

$$\hat{\Pi}_0(\boldsymbol{q},\omega) = 4\sum_{\lambda,\lambda',\boldsymbol{k}} |g_{\boldsymbol{k}}^{\lambda,\lambda'}(\boldsymbol{q})|^2 \frac{f[E_{\boldsymbol{k}+\boldsymbol{q}}^{\lambda'}]-f[E_{\boldsymbol{k}}^{\lambda}]}{\omega+E_{\boldsymbol{k}+\boldsymbol{q}}^{\lambda'}-E_{\boldsymbol{k}}^{\lambda}+i\delta}. \tag{4}$$

The factor 4 comes from the degenerate two spins and the two valleys at K and K'; and the vertex factor is $|g_{\boldsymbol{k}}^{\lambda,\lambda'}(\boldsymbol{q})|^2=[1+\lambda\lambda'\cos\alpha_{k+q}\cos\alpha_k+\lambda\lambda'\sin\alpha_{k+q}\sin\alpha_k(k+q\cos\theta)/|\boldsymbol{k}+\boldsymbol{q}|]/2$ with θ being the angle between $\boldsymbol{k}$ and $\boldsymbol{q}$. Since the intra-band backward scattering at $\boldsymbol{q}=2\boldsymbol{k}$ and the interband vertical transition at $\boldsymbol{q}=0$ are not allowed under Coulomb interaction in the system, we have $|g_{\boldsymbol{k}}^{\lambda,-\lambda}(0)|^2=|g_{\boldsymbol{k}}^{\lambda,\lambda}(2\boldsymbol{k})|^2=0$. The collective excitation spectrum is obtained by finding the zeros of the real part of the dielectric function ϵ_r. For convenience we denote each zero as a plasmon mode which may differ from the convention used in other places where some Landau damped modes are not counted since they do not have poles for $\hat{\epsilon}^{-1}$. In the following, we present our results using an estimated SOI strength $\sim$0.08–0.1 meV in graphene.[8] However, the results can easily be applied to Dirac gases of different Δ_{SO} by scaling the energy and wavevector in units of Δ_{SO} and $k_{\mathrm{SO}}=\Delta_{\mathrm{SO}}/(\hbar v)$, respectively. In graphene with the Fermi energy $E_F\gg\Delta_{\mathrm{SO}}$ (at the tempera-

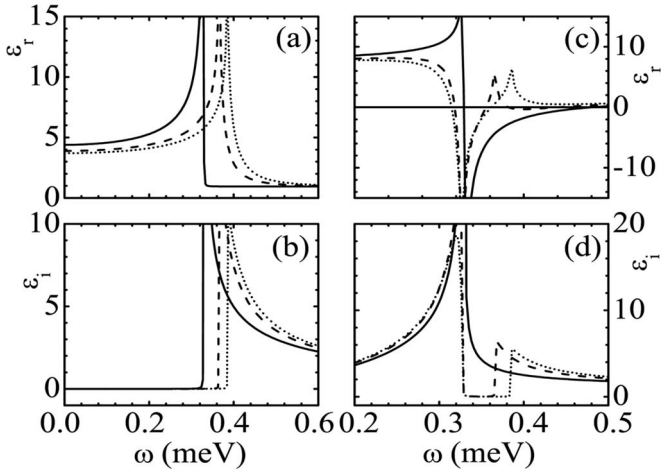

FIG. 1. Real (ϵ_r) and imaginary (ϵ_i) parts of the dielectric function vs ω at $T=0$ (left panels) and $T=2$ K (right panels) for an intrinsic graphene ($E_F=0$) and the SOI strength $\Delta_{SO}=0$ (solid), 0.08 meV (dashed), and 0.1 meV (dotted). The wave vector is $q=0.05\times10^5$ cm^{-1}.

ture $k_BT \gg \Delta_{SO}$), the SOI can be neglected. As a result, our $\Delta_{SO}=0$ result can be applied to systems of different carrier densities (temperatures) by scaling the energy and wavevector in units of the Fermi energy E_F (thermal energy k_BT) and wave vector $k_F=E_F/(\hbar v)$ $[k_T=k_BT/(\hbar v)]$, respectively.

First we explore the properties of an *intrinsic* graphene where the net electron density is zero and $E_F=0$. In Figs. 1(a) and 1(b), we show the real (ϵ_r) and imaginary (ϵ_i) parts of the dielectric function at $T=0$ for different SOI strengths[6,8] $\Delta_{SO}=0$ (solid), 0.08 (dashed), and 0.1 meV (dotted) at a wave vector $q=0.05\times10^5$ cm^{-1}. At $T=0$, only the interband transitions are allowed for electrons. The electron-hole propagator for $\Delta_{SO}=0$ is given by $\hat{\Pi}_0(\boldsymbol{q},\omega)=-q^2/[4\sqrt{\hbar^2v^2q^2-\omega^2}]$, which has been previously obtained via the renormalization group theory.[10,13] Therefore we have $\epsilon_r=1$ (for $\omega>\hbar vq$) above the interband electron-hole continuum (EHC) edge and $\epsilon_i=0$ (for $\omega<\hbar vq$) below it. With increasing Δ_{SO}, the peaks of ϵ_r and ϵ_i, which are located at the edge of the interband EHC, $\omega_H=2\sqrt{\Delta_{SO}^2+\hbar^2v^2q^2/4}$, shift to higher energies. At the same time, for $\omega>\omega_H$, ϵ_r increases continuously with Δ_{SO} and remains positive. As a consequence, in an intrinsic graphene there is no plasmon mode at zero temperature.

At a finite temperature, the intraband transitions are allowed and they contribute to the electron-hole propagator of Eq. (4) and a ϵ_r dip at the intraband EHC edge $\omega_L=\hbar vq$ is formed as shown in Fig. 1(c). For $\Delta_{SO}=0$, where $\omega_L=\omega_H$, two plasmon modes may appear: one strongly Landau damped at $\omega=\hbar vq$ while the other weakly damped at a higher energy. The damping rates of the plasmon modes are indicated in Fig. 1(d) by ϵ_i at the corresponding energies. Comparing the curves in Fig. 1(d) with those in 1(b) at a finite temperature we observe a finite ϵ_i at $\omega<\omega_L$ introduced by the intraband transition and a decreased ϵ_i for $\omega>\omega_L$ due to the weakening of the interband transitions, a result of the electronic occupation of the conduction band. With increasing Δ_{SO}, the ϵ_r peak shifts with ω_H to higher energies while

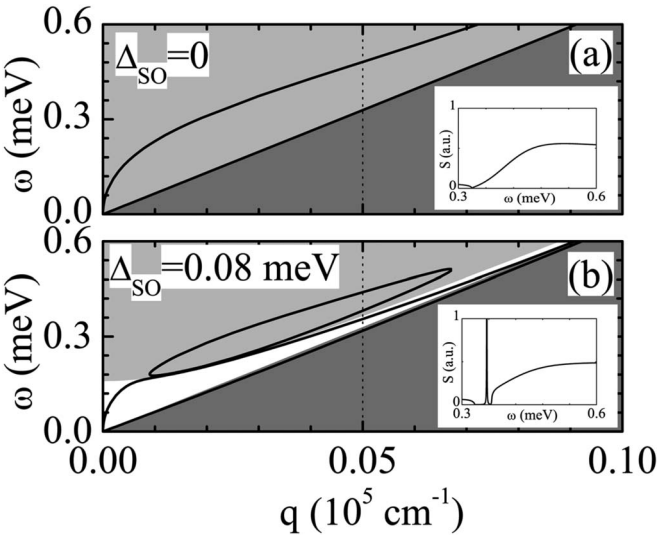

FIG. 2. Plasmon spectrum (thick curves) of an electron gas in an intrinsic graphene ($E_F=0$) at temperatures $T=2$ K with $\Delta_{SO}=0$ in (a) and 0.08 meV in (b). Intraband (dark shaded) and interband (light shaded) single-particle continuum are also shown. ω_L and ω_H are the lower and upper borders separating the white (EHC gap) and shaded areas, respectively, in (b). The vertical dotted lines indicate the q values for which excitation intensity is shown in the insets and the dielectric function is shown in Figs. 1(c) and 1(d).

the ϵ_r dip stays with ω_L. Since the ϵ_r peak has a lower energy than the ϵ_r dip initially at $\Delta_{SO}=0$, the peak and the dip merge at first and split again. As a result, at $T=2$ K the ϵ_r curve for $\Delta_{SO}=0.08$ meV is deformed in such a way that two extra zeros of ϵ_r or two new plasmon modes emerge [Fig. 1(c)]. Corresponding to the separation of the ϵ_r peak from its dip, the ϵ_i curve develops a gap between ω_L and ω_H as illustrated in Fig. 1(d). One of the plasmon modes is located in this ϵ_i gap or the EHC gap and is undamped, and can be observed experimentally. For $\Delta_{SO}=0.1$ meV, there is no damped plasmon mode in the interband EHC.

The appearance of the undamped plasmon mode in the presence of the SOI is a result of the interplay between the intraband and interband correlations which can be adjusted by varying the temperature of the system in experiments. For an intrinsic graphene with $\Delta_{SO}=0.08$ meV, increasing the temperature from $T=0$ the ratio of the intraband to the interband correlation increases and ϵ_r in the EHC gap ($\omega_L \leqslant \omega \leqslant \omega_H$) decreases and crosses zero. There is no plasmon mode when the interband correlation dominates at $T \leqslant 1.1$ K and only two damped modes exist when the intraband correlation dominates at $T \geqslant 3.3$ K. In the temperature region 1.1 K $\leqslant T \leqslant 3.3$ K or $T \approx 2\Delta_{SO}$ when the intraband and interband correlations match, however, $\epsilon_r(\omega_L)<0$ while $\epsilon_r(\omega_H)>0$ and one undamped plasmon mode exists. Furthermore, in the upper end of this regime at 1.9 K $\leqslant T \leqslant 3.3$ K, one undamped mode and three damped modes exist.

The ω versus q spectrum of the plasmon modes at $T=2$ K is plotted by thick solid curves for $\Delta_{SO}=0$ in Fig. 2(a) and for $\Delta_{SO}=0.08$ meV in Fig. 2(b). The weakly damped plasmon mode for $\Delta_{SO}=0$ has an approximate dispersion of $\omega \propto \sqrt{q}$ at small q. A finite Δ_{SO} separates ω_H from

ω_L and opens a gap between the intraband and interband EHC's. As a result, the formerly weakly damped plasmon mode becomes undamped near $q=0$ because it is now located in the gap. When it approaches the interband EHC edge, the dispersion curve of this mode is squeezed to a lower energy by the ϵ_r peak near the interband EHC edge as shown in Fig. 1(c) and then is split into three plasmon modes, viz., two new plasmon modes emerge near the interband EHC edge. One of the modes remain undamped in the EHC gap and the other Landau damped two are located inside the interband EHC. The latter two modes merge and disappear at q near 0.07×10^5 cm^{-1} for $\Delta_{SO}=0.08$ meV. The undamped mode survives at larger wavevectors until it merges with the strongly damped mode to the intraband EHC edge when the interband correlation dominates and ϵ_r becomes positive in the entire frequency regime. In the insets of Fig. 2, we show the excitation spectral weight or the dynamical structure factor $S(\mathbf{q},\omega)$ (Ref. 17) at $q=0.05\times10^5$ cm^{-1}. The damped plasmon spectral weight is hidden in the EHC's while the undamped plasmon spectrum appears as a sharp peak in the EHC spectral gap.[18,19]

As discussed above, the dominant intraband correlation results in the appearance of a plasmon mode with dispersion $\omega\propto\sqrt{q}$ at small q in the Dirac gases as well as in the Fermi gases.[20] Different from the normal Fermi gases, the Dirac gas at $E_F=0$ shows only the interband correlation at zero temperature and there is a strong competition between the intraband and interband correlations as the parameters of the system vary. Controlling the temperature of a graphene system we can change significantly the ratio between the intraband and interband many-body correlations of the Dirac electron gas with the SOI and this would lead to the observation of an undamped plasmon mode in the experiments. Another approach to changing the ratio between intraband and interband correlations is by varying the carrier density. By applying a gate voltage to a graphene layer or by doping one can manipulate the electron density and the Fermi energy in the system[1,2] and it would be interesting to observe the corresponding changes in the excitations.

Due to the symmetry of the band structure, systems having the same density of electrons or holes are equivalent. Here we consider a system with a net electron density and a positive Fermi energy E_F. For a Dirac gas in graphene, the extra electrons in the conduction band reduce the interband scattering rate but enhances the intraband one by increasing the length of the Fermi ring. Similar to the finite temperature case, a plasmon mode with an approximate dispersion $\omega\propto\sqrt{q}$ at small q appears even at zero temperature as shown in Fig. 3(a). For $\Delta_{SO}=0$ and at $T=0$, a EHC gap of width $2\hbar v(k_F-q)$ is opened above the intraband EHC edge in the range $0<q<k_F$. This EHC gap at the finite Fermi energy makes the $\omega\propto\sqrt{q}$ plasmon mode undamped near $q=0$. Another character of this mode at a finite fermi energy is its flat dispersion slope as shown by the dashed curve in Fig. 3(a), compared with the case at the finite temperature as shown in Fig. 2(a), near its entrance into the interband EHC. Furthermore, in contrast to the emergence of new plasmon modes occurred when its dispersion curve enters the interband EHC from a EHC gap due to the SOI, the dispersion curve enters the interband EHC smoothly here. In this paper, we characterize the carrier density by the Fermi energy to emphasize the interesting energy regime in the existence of SOI. The corresponding carrier density can be estimated with the help of their simple relation at zero temperature $n=(E_F^2-\Delta_{SO}^2)/(\pi v^2)$. For example, the carrier density of a system with $E_F=1$ meV is $n=7.34\times10^7$ cm^{-2}.

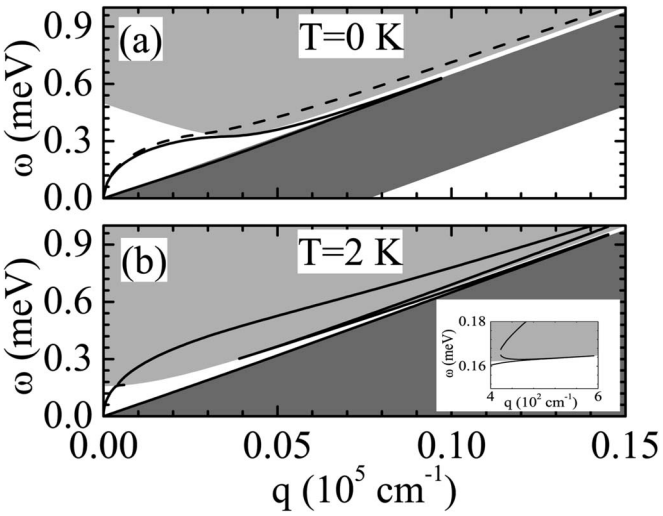

FIG. 3. The same as in Fig. 2 with $E_F=0.25$ meV at $T=0$ (a) and $T=2$ K (b). The solid curves are for $\Delta_{SO}=0.08$ meV and the dashed in (a) for $\Delta_{SO}=0$. In the inset of (b), we zoom the area where the $\sqrt{q}$ plasmon mode enters the interband EHC and splits into three modes.

The presence of the SOI changes the physical scenario of the excitation spectrum in the $\Delta_{SO}=0$ case described above. At $T=0$, the intraband EHC edge deviates from $\omega=\hbar vq$ to a lower energy $\sqrt{\Delta_{SO}^2+\hbar^2v^2(k_F+q)^2}-\sqrt{\Delta_{SO}^2+\hbar^2v^2k_F^2}$; the interband EHC edge shifts to a higher energy $\sqrt{\Delta_{SO}^2+\hbar^2v^2k_F^2}+\sqrt{\Delta_{SO}^2+\hbar^2v^2(k_F-q)^2}$ for $q<2k_F$ while remains ω_H when $q>2k_F$. More interestingly, the SOI may shift the plasmon mode in the interband EHC to the EHC gap and makes it undamped. For a system with $E_F=0.25$ meV, the plasmon mode at $q=0.05\times10^5$ cm^{-1} becomes undamped if $\Delta_{SO}>0.02$ meV. In a graphene with $\Delta_{SO}=0.08$ meV, the plasmon mode remains undamped up to $q=0.1\times10^5$ cm^{-1} where it merges with the mode in the intraband EHC as illustrated by the solid curves in Fig. 3(a).

At a finite temperature when the system is not degenerate, the restriction to single-particle transitions by the Fermi energy is relaxed and the EHC is independent of the Fermi energy as shown by the shades in Figs. 2(b) and 3(b). However, the collective excitation spectrum changes as the ratio of intraband to interband correlation increases with the net electron density. The relative weakening of interband correlation when $E_F>\Delta_{SO}$ lowers the ϵ_r peak at the interband EHC edge [Fig. 1(c)], and consequently changes the number or shifts the position of the zeros of ϵ_r for different q. Comparing the resulting plasmon spectrum in Fig. 3(b) with that in Fig. 2(b), we find that for q between $0.006-0.04\times10^5$ cm^{-1} the undamped mode disappears as the ϵ_r peak becomes less than zero and for q bigger than 0.07×10^5 cm^{-1} two damped modes exist in the interband EHC.

In summary, we have derived the electron-hole propagator and the dynamically screened Coulomb interaction matrix of an electron system in graphene with spin-orbit interaction in the RPA. In the intrinsic graphene without the SOI, our result reduces to the analytical result of a Dirac electron gas previously obtained by the renormalization group theory and predicts no collective excitations. The SOI changes the Dirac gas to a narrow gap semiconductor and splits the interband single-particle continuum from the intraband one. At a finite temperature or under an applied gate voltage, the intraband correlation introduces plasmon modes to the system and the interplay between the intraband and interband correlations plays an important role in the plasmon spectrum. More interestingly, an undamped plasmon mode exists in the EHC gap opened by the SOI in the wave-vector range of order 0.1×10^5 cm^{-1} and can be observed in the experiments.[18,19] Further, in a gated graphene with net electrons or holes, a EHC gap is formed for $q<k_F$ and an undamped plasmon mode of frequency $\omega\propto\sqrt{q}$ exists in the Dirac gas even at $T=0$ and with a negligible SOI, similar to the situation in a Fermi gas. In contrast to the negligible effect of the SOI to the dynamic Coulomb screening and the plasmon spectrum of a Fermi gas in a InGaAs quantum well,[21] however, the SOI may significantly change these properties of a Dirac gas in a graphene.

Recently, it has come to our attention that our zero-SOI result has been repeated by other authors[22] and our result has been employed to discuss the possibility of Wigner crystallization in graphene.[23]

One of the authors (X.F.W) thanks P. Vasilopoulos for helpful discussions. The work has been supported by the Canada Research Chair Program and a Canadian Foundation for Innovation (CFI) Grant.

*Electronic address: tapash@physics.umanitoba.ca

[1] K. S. Novoselov *et al.*, Nature (London) **438**, 197 (2005).
[2] Y. Zhang, Y. W. Tan, H. L. Stormer, and P. Kim, Nature (London) **438**, 201 (2005).
[3] Y. Zhang *et al.*, Phys. Rev. Lett. **96**, 136806 (2006).
[4] M. Wilson, Phys. Today **59** (1), 21 (2006).
[5] P. R. Wallace, Phys. Rev. **71**, 622 (1947); J. C. Slonczewski and P. R. Weiss, *ibid.* **109**, 272 (1958).
[6] T. Ando, in *Nano-physics & Bio-electronics: A New Odyssey*, edited by T. Chakraborty, F. Peeters, and U. Sivan (Elsevier, Amsterdam, 2002), Chap. 1.
[7] G. W. Semenoff, Phys. Rev. Lett. **53**, 2449 (1984); F. D. M. Haldane, *ibid.* **61**, 2015 (1988).
[8] C. L. Kane and E. J. Mele, Phys. Rev. Lett. **95**, 226801 (2005); D. P. DiVincenzo and E. J. Mele, Phys. Rev. B **29**, 1685 (1984).
[9] N. A. Sinitsyn, J. E. Hill, H. Min, J. Sinova, and A. H. MacDonald, Phys. Rev. Lett. **97**, 106804 (2006).
[10] D. V. Khveshchenko, Phys. Rev. B **74**, 161402(R) (2006).
[11] N. M. R. Peres, F. Guinea, and A. H. Castro Neto, Phys. Rev. B **72**, 174406 (2005); J. Nilsson, A. H. Castro Neto, N. M. R. Peres, and F. Guinea, *ibid.* **73**, 214418 (2006).
[12] T. Ando, J. Phys. Soc. Jpn. **69**, 1757 (2000); T. Ando (unpublished).
[13] J. González, F. Guinea, and M. A. H. Vozmediano, Nucl. Phys. B **424**, 595 (1994); Phys. Rev. B **59**, R2474 (1999); **63**, 134421 (2001).
[14] J. V. Alvarez and G. G. N. Angilella, Solid State Commun. **132**, 683 (2004).
[15] O. Vafek, Phys. Rev. Lett. **97**, 266406 (2006).
[16] B. Vinter, Phys. Rev. B **15**, 3947 (1977).
[17] S. Das Sarma and E. H. Hwang, Phys. Rev. Lett. **81**, 4216 (1998).
[18] C. C. Grimes and G. Adams, Phys. Rev. Lett. **36**, 145 (1976); S. J. Allen, Jr., D. C. Tsui, and R. A. Logan, *ibid.* **38**, 980 (1977).
[19] A. Pinczuk, M. G. Lamont, and A. C. Gossard, Phys. Rev. Lett. **56**, 2092 (1986); G. Fasol, N. Mestres, H. P. Hughes, A. Fischer, and K. Ploog, *ibid.* **56**, 2517 (1986).
[20] F. Stern, Phys. Rev. Lett. **18**, 546 (1967).
[21] X. F. Wang, Phys. Rev. B **72**, 085317 (2005).
[22] E. H. Hwang and S. Das Sarma, cond-mat/0610561 (unpublished).
[23] H. P. Dahal, Y. N. Joglekar, K. S. Bedell, and A. V. Balatsky, Phys. Rev. B **74**, 233405 (2006).